

Carotid Plaque Vulnerability Assessment Using Ultrasound Elastography and Echogenicity Analysis

Guy Cloutier^{1,2}
 Marie-Hélène Roy Cardinal¹
 Yang Ju³
 Marie-France Giroux³
 Sylvain Lanthier^{4,5}
 Gilles Soulez^{2,3,6}

Keywords: carotid artery, patients with symptomatic ischemia, sonography, ultrasound echogenicity, ultrasound elastography

doi.org/10.2214/AJR.17.19211

Received October 26, 2017; accepted after revision March 22, 2018.

Supported by grant PPP-78763 from the Canadian Institutes of Health Research (CIHR) and by maturation funding from Univalor, for acquisition of imaging data, and by grants STPGP-381136-09, DG-138570-11, and CHRP-462240-2014 from the Natural Sciences and Engineering Research Council of Canada and by grant CPG-134748 from CIHR, for technical developments and data analysis.

¹Laboratory of Biorheology and Medical Ultrasonics, University of Montreal Hospital Research Center (CRCHUM), 900 Saint-Denis, Rm R11-464, Montreal, QC H2X 0A9, Canada. Address correspondence to G. Cloutier (guy.cloutier@umontreal.ca).

²Department of Radiology, Radio-Oncology and Nuclear Medicine, and Institute of Biomedical Engineering, University of Montreal, Montreal, QC, Canada.

³Department of Radiology, University of Montreal Hospital (CHUM), Montreal, QC, Canada.

⁴Department of Neurosciences, University of Montreal, Montreal, QC, Canada.

⁵Department of Neurology, CHUM, Montreal, QC, Canada.

⁶Laboratory of Clinical Image Processing, CRCHUM, Montreal, QC, Canada.

Supplemental Data
 Available online at www.ajronline.org.

AJR 2018; 211:847–855

0361–803X/18/2114–847

© American Roentgen Ray Society

OBJECTIVE. The purpose of this study was to evaluate ultrasound elastography and echogenicity analysis to discriminate between carotid plaques in patients with symptomatic internal carotid artery (ICA) stenosis versus patients with asymptomatic stenosis.

SUBJECTS AND METHODS. Patients with symptomatic and asymptomatic ICA stenosis of more than 50% were recruited for the study. After both carotid arteries were scanned, plaque translation and elastography and echogenicity features were assessed. Parameters of index stenosis (i.e., symptomatic or more severe stenosis) were compared between populations. For further validation, parameters of index stenosis were also compared with those of the contralateral artery for segments with plaque. Segments without plaque on the index side were also evaluated between populations. ROC curve analyses were performed using a cross-validation method with bootstrapping to calculate sensitivity and specificity.

RESULTS. Sixty-six patients with symptomatic ($n = 26$) or asymptomatic ($n = 40$) carotid stenoses were included. The maximum axial strain ($p < 0.001$), maximum axial shear strain magnitude ($p = 0.03$), and percentage of low-intensity of gray level ($p = 0.01$) of the index ICA were lower for patients with symptoms than for those without symptoms. In both groups, the contralateral ICA had translation and elastography and echogenicity parameters similar to those of the index ICA in patients with asymptomatic stenosis. The ROC curve for the detection of vulnerable plaques in patients with symptomatic stenosis was higher when ultrasound elastography and ultrasound echogenicity were used in combination than when each method was used alone ($p < 0.001$); a sensitivity of 71.6% and a specificity of 79.3% were obtained.

CONCLUSION. This pilot study establishes the usefulness of combining elastography with echogenicity analysis to discriminate plaques in patients with symptomatic ICA stenosis versus asymptomatic stenosis.

Atherosclerosis is an inflammatory and healing response of the arterial wall. Confluence of foam cells within the artery wall leads to a plaque formation [1]. Plaque vulnerability depends on tissue composition, inflammation, neovascularization, intraplaque hemorrhage, surface characteristics, and biomechanical properties [2]. Ruptured plaques are usually characterized in histologic analysis by a lipid core under a thin fibrous cap infiltrated by macrophages [3–5]. With the use of ultrasound, a variety of carotid biomarkers have been studied to identify the features associated with unstable plaques. The carotid artery intima-media thickness is a predictor of premature carotid atherosclerosis, but its association with stroke risk has been denied in the general population [6, 7]. Contrast-enhanced ultrasound can detect the vasa vaso-

rum neovascularization of carotid plaques [8]. The B-mode ultrasound echotexture [9, 10] and plaque volume [11, 12] were used to evaluate carotid plaque vulnerability, predict future cardiovascular events, and determine plaque regression with statin therapy.

Ultrasound-based mechanical parameters assessing vessel wall motion and plaque deformation were also proposed. Small longitudinal translations (displacements) of the common carotid wall were associated with greater occurrence of myocardial ischemia [13] and established cardiovascular risk factors [14]. Internal carotid artery (ICA) strain imaging or elastography was correlated with plaque lipid content determined by MRI [15] and could differentiate vulnerable plaques from fibrous plaques assessed by histologic analysis [16]. Application of this ultrasound method to unstable plaques could identify

fy patients with symptomatic ICA stenosis with poorer cognitive performance presumably related to carotid emboli in silent stroke [17]. Low-echogenic plaques attributed to the presence of lipid [18] have long been related to symptoms in various studies [19, 20]. The presence of such plaques could also predict stroke in patients with asymptomatic stenosis [21]. Moreover, plaque texture features could differentiate symptomatic from asymptomatic carotid artery plaques [22].

The purpose of the present study was to evaluate computerized methods of measuring plaque echogenicity and to determine whether mechanical biomarkers (e.g., translation motion, strain, and shear) assessed using ultrasound elastography could be associated with symptoms of ischemia in patients with atherosclerotic ICA stenosis. This study combines analysis of echogenicity and plaque mechanical properties to compare patterns observed in ipsilateral and index plaques and ICA wall segments without plaques in patients with symptomatic or asymptomatic stenosis as well as in plaques of the contralateral arteries.

Subjects and Methods

This prospective cross-sectional study was HIPAA compliant and received institutional review board approval. Written informed consent was obtained from all participants.

Recruitment

Men and women (age range, 40–90 years) with ICA diameter reduction of at least 50% (as defined by Doppler ultrasound) [23] were eligible for inclusion. Exclusion criteria included the presence of severe vascular calcifications that impeded Doppler imaging and ICA for which radiotherapy of the neck region, endarterectomy, or stenting had previously occurred.

Individuals with a clinical indication for ICA imaging from the vascular and interventional radiology, vascular surgery, neurology, and vascular medicine departments at the University of Montreal Hospital were approached from April 2005 to December 2010. Clinical indications for imaging included new-onset ischemic cerebrovascular symptoms, incidental findings of ischemic disease on brain imaging, and screening in the setting of peripheral vascular diseases. Recruited participants were classified as having symptomatic or asymptomatic ICA stenosis. To be considered as having symptomatic stenosis, a patient had to have reported a neurologic symptom solely attributable to the ipsilateral ICA within 3 months before the study enrollment date. If doubts existed as to the

presence of symptoms, the patient was referred to a neurologist for confirmation of symptoms. A detailed medical questionnaire was completed, and physical examination was performed for all participants at the time of enrollment.

A total of seventy-three participants met all the inclusion criteria. Seven were excluded for the following reasons: previous neck radiotherapy on the ICA side studied ($n = 3$), poor-quality elastography images ($n = 2$), severe plaque calcifications ($n = 1$), and plaque instability and the urgent need for surgical intervention before examination ($n = 1$). Nine of 26 individuals with symptoms (35%) and 22 of 40 individuals without symptoms (55%) were previously included in a study of ultrasound elastography versus MRI [15].

Ultrasound Data Acquisition

Both ICAs were examined in each participant. The index ICA corresponded to the ipsilateral side for patients with symptoms and to the side with greatest stenosis for individuals without symptoms. The contralateral asymptomatic or less-stenosed ICA was used as the comparator for intrapatient validation of plaque vulnerability criteria. ICA segments without stenosis were also compared between populations.

A duplex color and pulsed Doppler ultrasound examination, followed by radiofrequency image acquisitions, was performed for all participants at enrollment by either of two participating radiologists who had more than 10 years and more than 20 years of experience in vascular imaging. Two-dimensional duplex ultrasound recordings in the longitudinal view of the ICA were acquired using an HDI 5000 ultrasound system (Philips Healthcare). The latter examination aimed to identify diseased artery segments and grade the severity of the stenosis. The percentage of stenosis was evaluated using ultrasound velocity profiles (the peak systolic velocity in the ICA and the ratio of the peak systolic velocity of the ICA to the peak systolic velocity of the common carotid artery) [23]. The Doppler resistivity index was also determined for the common carotid artery segment on the index side. The 2D radiofrequency data were then acquired using an advanced ultrasound research platform (ES500RP, Ultrasonix) equipped with an L14–5/38 10-MHz linear array. Radiofrequency loop sequences were acquired longitudinally at the carotid bulb and at the distal ICA for more than approximately 10 seconds. Blood pressure measured on the left forearm was recorded immediately before and after ultrasound image acquisitions, and the mean value was reported. Radiofrequency data were processed offline with use of a computer platform developed in-house.

Image Analysis

The ultrasound radiofrequency data-processing algorithms were implemented using a commercial imaging platform (Visual-NIVE, Object Research Systems). A specific set of processing steps was followed. First, a B-mode cine loop was reconstructed from radiofrequency images with use of standard Hilbert transformation and logarithm compression. Then, carotid plaques were manually segmented on a B-mode image frame selected from the cine loop, to initialize an automated segmentation of all remaining frames. Good agreement was reported with this algorithm when compared with results for reference standard manual segmentations of 8988 images on 94 cine loops from 33 patients [24]. All segmentations were done by a technician and a third-year diagnostic radiology resident and were then verified by the radiologist who had more than 20 years of experience in vascular imaging. If doubt existed because of suboptimal radiofrequency image quality, Doppler-duplex images were consulted to help with segmentation. Carotid wall segments without plaque were segmented with the validated method of Destrempe et al. [25]. All professionals involved in the study were blinded to elastography and echogenicity results.

Elastograms were generated for each pair of time-varying radiofrequency images to assess the mechanical properties of the segmented plaque or carotid wall without plaque induced by natural cardiac pulsation [15, 26]. Elastography cine loops of axial and lateral translation motions, axial strains, and axial shear strains were computed (“axial” was used to denote the direction of the ultrasound beam, and “lateral” referred to the direction perpendicular to the ultrasound beam). For each mechanical parameter, the spatial average over the segmented region was calculated and displayed as a function of time over consecutive cardiac cycles. Descriptive imaging biomarkers were extracted from these elastography time-varying curves—namely, cumulated axial translation, cumulated lateral translation, maximum and cumulated axial strains, and maximum and cumulated axial shear strain magnitudes. Cumulated indexes were calculated by adding instantaneous measures (values were reset to zero at each cardiac cycle) and by taking the range of variation over a cycle. Maximum indexes correspond to the highest value within a cycle. For the whole dataset, imaging biomarkers were averaged over a mean (\pm SD) of 5.3 ± 1.7 cardiac cycles. Figures 1 and 2 show examples of elastograms and time-varying biomarkers for a patient with symptomatic ICA stenosis and a patient with asymptomatic ICA stenosis, respectively.

Echogenicity parameters were determined for segmented carotid plaque or carotid wall without plaque on reconstructed B-mode images. Be-

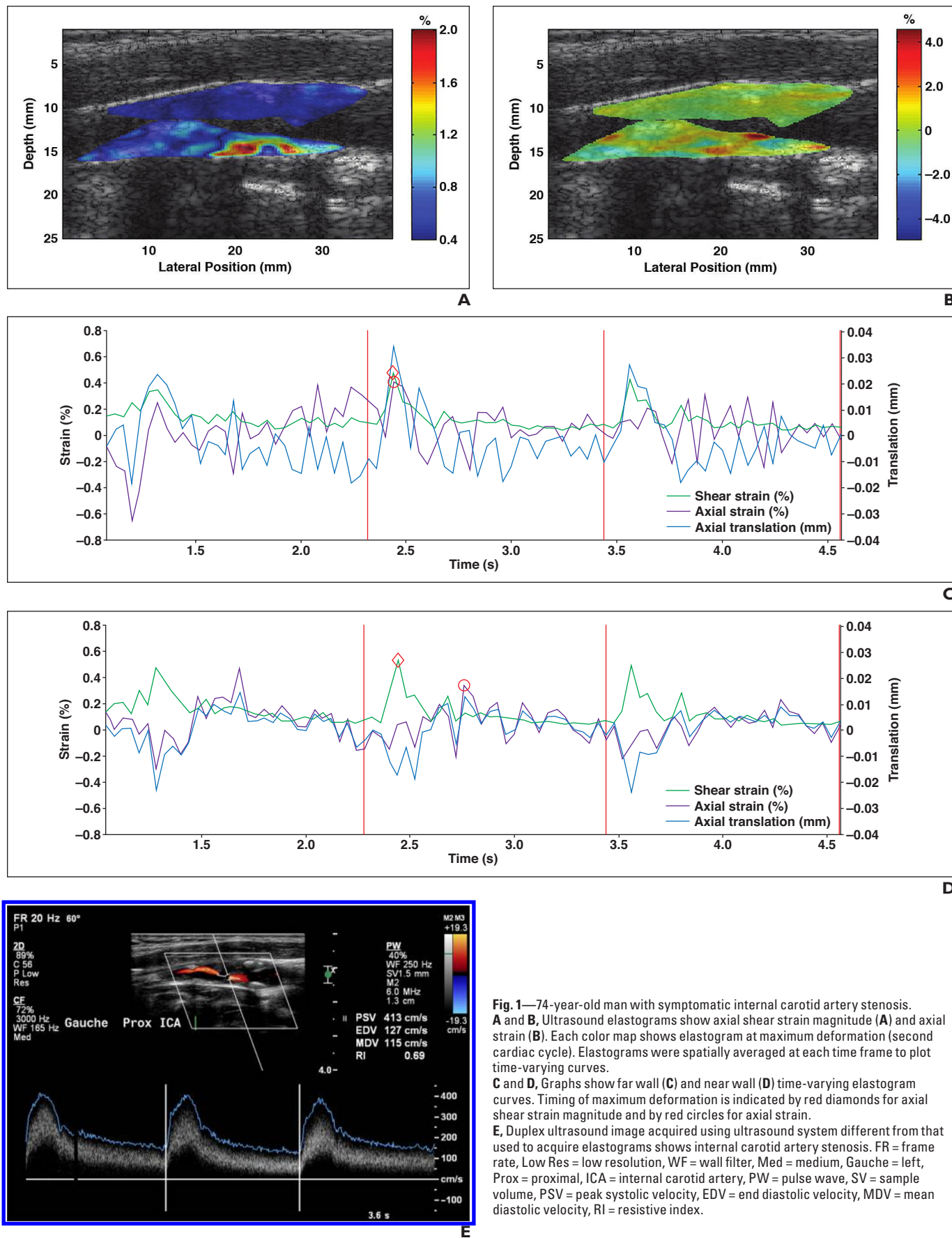


Fig. 1—74-year-old man with symptomatic internal carotid artery stenosis. **A** and **B**, Ultrasound elastograms show axial shear strain magnitude (**A**) and axial strain (**B**). Each color map shows elastogram at maximum deformation (second cardiac cycle). Elastograms were spatially averaged to plot time-varying curves. **C** and **D**, Graphs show far wall (**C**) and near wall (**D**) time-varying elastogram curves. Timing of maximum deformation is indicated by red diamonds for axial shear strain magnitude and by red circles for axial strain. **E**, Duplex ultrasound image acquired using ultrasound system different from that used to acquire elastograms shows internal carotid artery stenosis. FR = frame rate, Low Res = low resolution, WF = wall filter, Med = medium, Gauche = left, Prox = proximal, ICA = internal carotid artery, PW = pulse wave, SV = sample volume, PSV = peak systolic velocity, EDV = end diastolic velocity, MDV = mean diastolic velocity, RI = resistive index.

for echogenicity analysis, image normalization was performed as described elsewhere [27]. Linear scaling was applied by assigning the value 0 to the lowest gray level in the blood region and the value 190 to the highest gray level in the adventi-

tia. The blood region was defined as a 3-mm-thick space located inside the lumen and adjacent to the lumen-plaque segmentation contour. The adventitia region was selected as a 3-mm-thick space located outside the vessel wall and adjacent to the

plaque-adventitia segmentation. Selected computerized echogenicity parameters included the mean gray level, the percentage of low-intensity gray levels, and the percentage of high-intensity gray levels. The percentage of low-intensity gray lev-

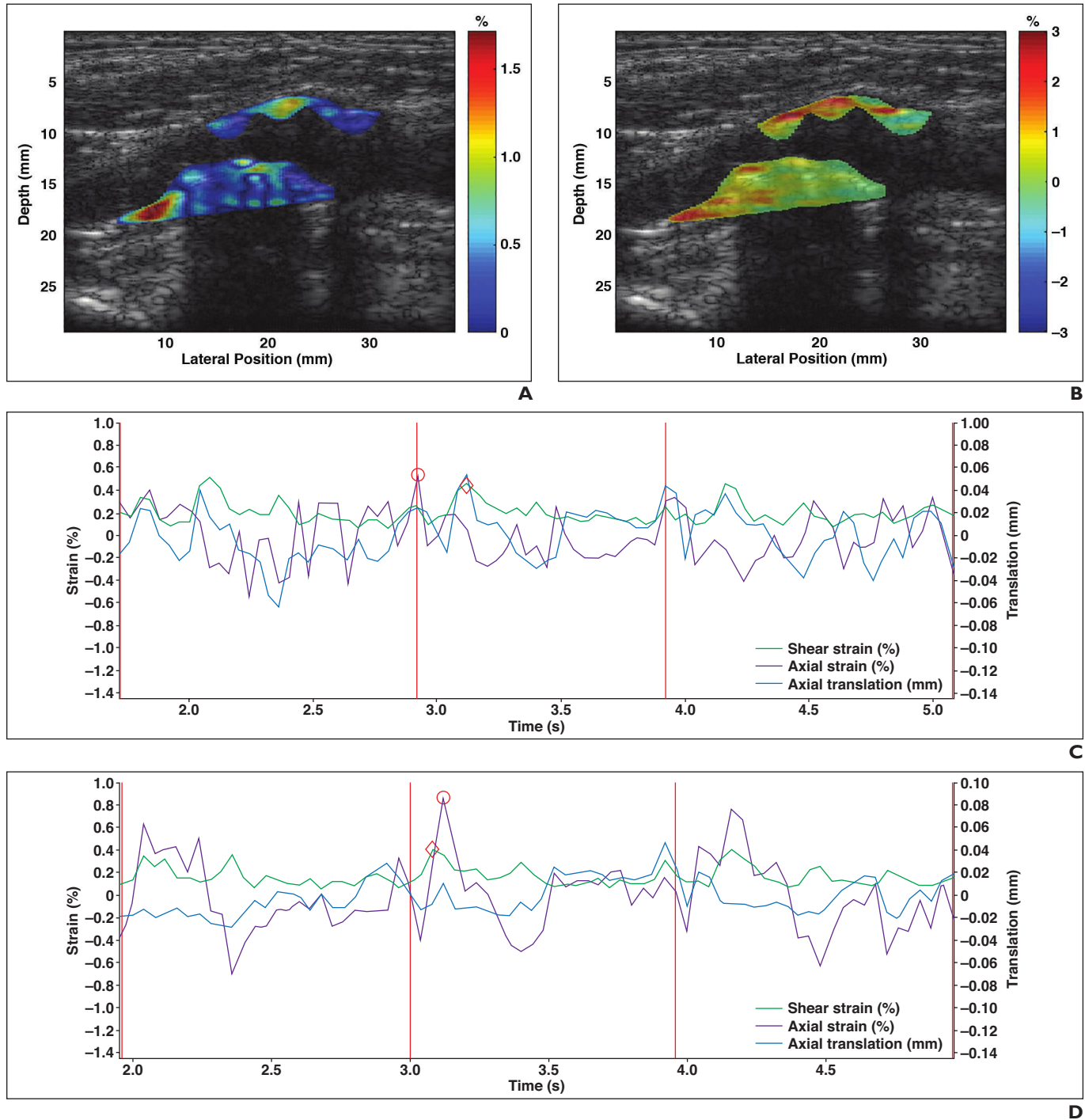


Fig. 2—68-year-old man with asymptomatic internal carotid artery stenosis. **A** and **B**, Ultrasound elastograms show axial shear strain magnitude (**A**) and axial strain (**B**). Each color map shows elastogram at maximum deformation (second cardiac cycle). Elastograms were spatially averaged at each time frame to plot time-varying curves. **C** and **D**, Graphs show far wall (**C**) and near wall (**D**) time-varying elastogram curves at maximum deformation (second cardiac cycle). Timing of maximum deformation is indicated by red diamonds for axial shear strain magnitude and by red circles for axial strain.

(Fig. 2 continues on next page)

US Elastography and Echogenicity Analysis of ICA Plaques

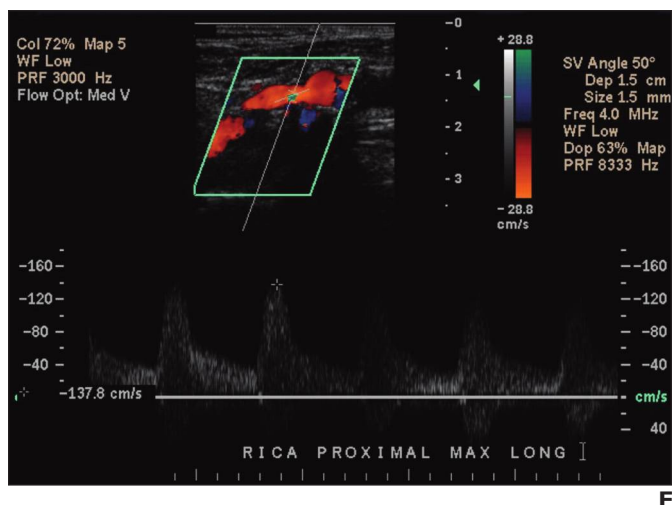


Fig. 2 (continued)—68-year-old man with asymptomatic internal carotid artery stenosis. **E**, Duplex ultrasound image acquired using ultrasound system different from that used to acquire elastograms shows internal carotid artery stenosis. Col = color, WF = wall filter, PRF = pulse repetition frequency, SV = sample volume, Dep = depth, Freq = frequency, WF = wall filter, Dop = Doppler, RICA = right internal carotid artery, Max = site of maximum stenosis, LONG = longitudinal value.

els and the percentage of high-intensity gray levels correspond, respectively, to pixel values of less than 75 and higher than 150, after normalization. Echogenicity parameters were computed over all segmented frames of the approximately 10-second sequence and were averaged over time.

Statistical Analyses

Results are presented as mean (\pm SD) values. Data were tested for normality with use of the Shapiro-Wilk test. The Pearson chi-square test with Yates correction for continuity or the Fisher exact test was used to compare categorical variables. Continuous variables (physiologic parameters and plaque biomarkers) were compared between patients with symptomatic and asymptomatic ICA stenosis with the use of unpaired *t* tests or Mann-Whitney tests when applicable. Paired tests were used to compare the index and contralateral sides in both patient groups. Principal components analysis (PCA) was applied to elastography and echogenicity variables. ROC curves were used to determine the accuracy of selected PCA variables and single biomarkers to detect symptoms. ROC curves were calculated using a cross-validation method using the 0.632+ bootstrap algorithm (1000 bootstrap samples) [28]. Nonparametric CIs were computed for AUC values with the use of a leave-one-patient-out method; in this case, the 0.632+ bootstrap algorithm was applied to each leave-one-patient-out sample. The AUC values of PCA and single biomarkers were compared using Wilcoxon signed rank tests.

Results

Population Characteristics

As shown in Table 1, 66 participants were included in final data analysis, including 47 men (71%) and 19 women (29%) 49–86 years old (mean age, 70.1 ± 8.2 years). In 26 participants (39%) with symptomatic stenosis, the ischemic

manifestations were as follows: stroke ($n = 12$; 46%), amaurosis fugax ($n = 7$; 27%), transient ischemic attack ($n = 6$; 23%), and retinal infarct ($n = 1$; 4%). The mean elapsed time be-

tween symptom onset and acquisition of ultrasound scans was 22 ± 42 days.

The degree of index stenosis ranged from 50% to near occlusion (mean, $73.3\% \pm 14.1\%$). No differences in index stenosis severity and the pulsatility index were found between patients with symptomatic stenosis and patients with asymptomatic stenosis ($p = 0.642$ and $p = 0.919$) (Table 1). The degree of stenosis on the contralateral sides was $25.4\% \pm 19.7\%$; it was assessed in 20 patients with symptomatic stenosis and 22 patients with asymptomatic stenosis. For the contralateral side, six patients with symptomatic stenosis could not be included because of poor image quality ($n = 2$), absence of plaque ($n = 1$), presence of thrombosis ($n = 1$), prior stroke associated with this side ($n = 1$), and radiotherapy in the neck region on this side ($n = 1$). For patients with asymptomatic stenosis, 18 contralateral sides were excluded because of prior stroke, carotid endarterectomy, or stenting on this

TABLE 1: Study Population Characteristics

Characteristic	All Patients ($n = 66$)	Patients With Symptoms ($n = 26$)	Patients Without Symptoms ($n = 40$)	<i>p</i>
Male sex, no. (%) of patients ^a	47 (71.2)	21 (80.8)	26 (65.0)	0.269
Age (y), mean \pm SD ^b	70.1 ± 8.2	70.5 ± 8.5	69.8 ± 8.0	0.875
BMI ^c	26.4 ± 4.0	27.2 ± 4.7	25.8 ± 3.4	0.157
Peripheral vascular disease, no. (%) of patients ^a	39 (59.1)	9 (34.6)	30 (75.0)	0.003 ^d
Ischemic heart disease, no. (%) of patients ^a	28 (42.2)	8 (30.8)	20 (50.0)	0.197
Treatment received, no. (%) of patients				
For diabetes mellitus ^a	21 (31.8)	7 (26.9)	14 (35.0)	0.676
For dyslipidemia ^e	54 (81.8)	17 (65.4)	37 (92.5)	0.008 ^d
For hypertension ^e	56 (84.8)	20 (76.9)	36 (90.0)	0.175
Smoking history, no. (%) of patients ^e	56 (84.8)	23 (88.5)	33 (82.5)	0.728
SBP (mm Hg) ^b	135.2 ± 15.6	133.2 ± 14.2	136.5 ± 16.5	0.409
DBP (mm Hg) ^b	71.2 ± 10.0	72.9 ± 10.3	70.0 ± 9.8	0.249
Heartbeat (beats/min) ^b	74.1 ± 15.3	77.1 ± 17.0	72.0 ± 13.9	0.249
Stenosis severity of index side (%) ^c	73.3 ± 14.1^f	74.5 ± 14.7^g	72.6 ± 13.7^h	0.642
Doppler resistivity index ^c	0.76 ± 0.07	0.76 ± 0.08	0.76 ± 0.07	0.919

Note—Except where otherwise indicated, data are mean (\pm SD) values. BMI = body mass index (weight in kilograms divided by the square of height in meters), SBP = systolic blood pressure, DBP = diastolic blood pressure.

^aBy Pearson chi-square test with Yates correction for continuity.

^bBy Mann-Whitney rank sum test.

^cBy *t* test.

^dStatistically significant ($p < 0.05$).

^eBy Fisher exact test.

^fForty-three patients had stenosis severity $\geq 70\%$.

^gSeventeen patients had stenosis severity $\geq 70\%$.

^hTwenty-six patients had stenosis severity $\geq 70\%$.

TABLE 2: Overview of Elastography Indexes Obtained From Plaques on Both Index and Contralateral Sides of Patients With Symptomatic or Asymptomatic Internal Carotid Artery Stenosis

Mechanical Parameter	Patients With Symptomatic Stenosis		Patients With Asymptomatic Stenosis		<i>p</i>		
	Index Side (<i>n</i> = 26)	Contralateral Side (<i>n</i> = 20)	Index Side (<i>n</i> = 40)	Contralateral Side (<i>n</i> = 22)	Index Sides ^a	Symptomatic Stenosis ^b	Asymptomatic Stenosis ^c
Cumulated axial translation (mm)	0.27 ± 0.20	0.27 ± 0.14	0.29 ± 0.17	0.28 ± 0.24	0.408	0.895	0.871
Cumulated lateral translation (mm)	0.40 ± 0.33	0.40 ± 0.23	0.37 ± 0.23	0.37 ± 0.22	0.723	0.267	0.700
Maximum axial strain (%)	0.42 ± 0.22	0.58 ± 0.31	0.57 ± 0.19	0.58 ± 0.25	< 0.001 ^d	0.019 ^d	0.498
Cumulated axial strain (%)	1.41 ± 0.86	1.99 ± 1.24	1.87 ± 0.66	1.78 ± 0.79	0.005 ^d	0.014 ^d	0.808
Maximum axial shear strain magnitude (%)	0.63 ± 0.15	0.67 ± 0.20	0.71 ± 0.15	0.72 ± 0.21	0.030 ^d	0.898	0.417
Cumulated axial shear strain magnitude (%)	5.76 ± 2.18	5.25 ± 1.27	5.75 ± 1.60	5.70 ± 1.95	0.555	0.898	0.941

Note—Except where otherwise indicated, data are mean (± SD) values.

^aComparison of index sides of patients with symptomatic stenosis versus those with asymptomatic stenosis, as assessed using *t* tests.

^bComparison of index versus contralateral sides of patients with symptomatic stenosis, as assessed using paired *t* tests.

^cComparison of index versus contralateral sides of patients with asymptomatic stenosis, as assessed using paired *t* tests.

^dStatistically significant (*p* < 0.05).

side (*n* = 12); absence of plaque (*n* = 3); and presence of complete occlusion (*n* = 3). No statistically significant difference existed between the degree of stenosis on the contralateral sides (24.0% ± 16.3% and 26.6% ± 26.6%, for patients with symptomatic stenosis and asymptomatic stenosis, respectively; *p* = 0.851). As is shown in Table 1, no statistically significant difference was noted in the number of subjects treated for diabetes mellitus or hypertension in both groups (*p* > 0.175); however, patients who received treatment for dyslipidemia comprised a higher proportion of the group with asymptomatic stenosis (*p* = 0.008) (Table 1).

Ultrasound Elastography Analysis

Table 2 presents elastography indexes obtained from plaques on the index and contralateral sides of patients with symptomatic and asymptomatic stenosis. Lower axial strains (maximum axial strain and cumulated axial strain) and shear (maximum ax-

ial shear strain magnitude) were noticed on index side of patients with symptomatic stenosis (*p* < 0.001–0.03), in comparison with index side of individuals with asymptomatic stenosis. Axial strain indexes also differed between the index and contralateral sides of patients with symptomatic stenosis (maximum axial strain, *p* = 0.019; cumulated axial strain, *p* = 0.014). Cumulated axial and lateral translations had no discriminating value. No differences in any parameter were noticed between the index and contralateral sides of patients with asymptomatic stenosis. Appendix S1 and Table S2 (which can be viewed in the *AJR* electronic supplement to this article, available at www.ajronline.org) provides comparisons of elastography measures between stenotic-free segments of the index ICA between populations.

Ultrasound Echogenicity Analysis

All echogenicity indexes could discriminate between index plaques of patients with

symptomatic and asymptomatic stenosis (*p* < 0.039) (Table 3). Symptoms were associated with a lower mean gray level, a lower percentage of high-intensity gray level, and a higher percentage of low-intensity gray level. A larger proportion of low-intensity pixels was also noticed in the index versus the contralateral sides of patients with symptomatic stenosis (*p* = 0.028). A higher percentage of low-intensity gray level on the ipsilateral side, which differs from the contralateral side of patients with symptomatic stenosis and from both sides of patients with asymptomatic stenosis, reflects the vulnerable status of those plaques. No differences in any parameter were observed between the index and contralateral sides of patients with asymptomatic stenosis. Table S2 also compares echogenicity indexes between stenotic-free segments of the index ICA between populations. Table S3 (which can be viewed in the *AJR* electronic supplement to this article, available at www.ajronline.org) presents

TABLE 3: Overview of Echogenicity Indexes Obtained From Plaques on Both Index and Contralateral Sides of Patients With Symptomatic or Asymptomatic Internal Carotid Artery Stenosis

Echogenicity Parameter	Patients With Symptomatic Stenosis		Patients With Asymptomatic Stenosis		<i>p</i>		
	Index Side (<i>n</i> = 26)	Contralateral Side (<i>n</i> = 20)	Index Side (<i>n</i> = 40)	Contralateral Side (<i>n</i> = 22)	Index Sides ^a	Symptomatic Stenosis ^b	Asymptomatic Stenosis ^c
Mean gray level ^d	89.1 ± 20.3	96.1 ± 19.2	97.2 ± 16.5	99.0 ± 18.2	0.039 ^e	0.211	0.925
Percentage of low-intensity gray level	41.2 ± 22.0	29.6 ± 18.5	29.2 ± 14.6	27.9 ± 15.5	0.010 ^e	0.028 ^e	0.882
Percentage of high-intensity gray level	6.6 ± 9.8	9.2 ± 10.0	9.5 ± 8.9	10.9 ± 12.0	0.033 ^e	0.245	0.779

Note—Except where otherwise indicated, data are mean (± SD) values.

^aComparison of index sides of patients with symptomatic stenosis versus those with asymptomatic stenosis, as assessed using *t* tests.

^bComparison of index versus contralateral sides of patients with symptomatic stenosis, as assessed using paired *t* tests.

^cComparison of index versus contralateral sides of patients with asymptomatic stenosis, as assessed using paired *t* tests.

^dUsing an intensity scale of 0–190.

^eStatistically significant (*p* < 0.05).

US Elastography and Echogenicity Analysis of ICA Plaques

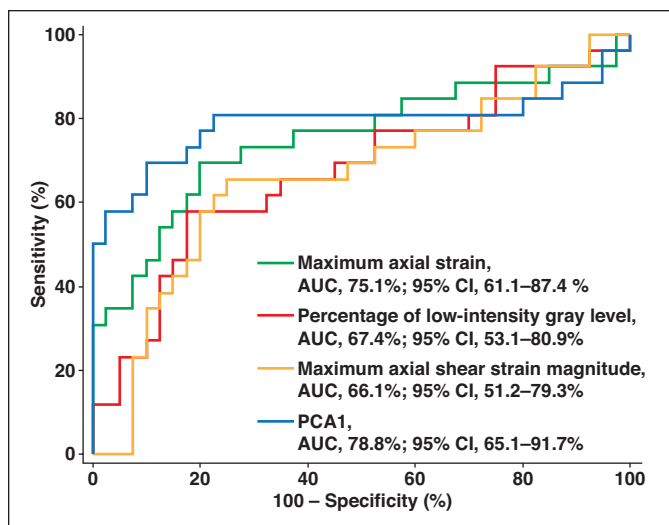


Fig. 3—ROC curves to detect symptoms based on maximum axial strain (green curve), percentage of low-intensity gray levels (red curve), maximum axial shear strain magnitude (orange curve), and combination of those three parameters using principal component analysis model 1 (PCA1, blue curve). CI is based on leave-one-patient-out bootstrapping method.

correlations between elastography and echogenicity features from the whole database for index plaques.

Classification Performance

Because of similarities in the definition of biomarkers within a given category (i.e., cumulated axial or lateral translation, maximum or cumulated strain and shear, and three measures of echogenicity), the most discriminating parameter in any category (Tables 3 and 4) was selected for classification. As is illustrated in Figure 3, for discriminating symptoms, the accuracy provided by ROC analyses was 71.0% with maximum axial strain (sensitivity, 58.3%; specificity, 78.7%), 63.0% with the percentage of low-intensity gray level (sensitivity, 52.6%; specificity, 70.4%), and 62.0% with the maximum axial shear strain magnitude (sensitivity, 53.3%; specificity, 71.8%) when single parameters were considered. By linearly combining those parameters in the framework of a PCA, the accuracy of ROC analysis increased to 78.0% (sensitivity, 71.6%; specificity, 79.3%). The multiparametric model discriminating between both populations ($p < 0.001$) and explaining 43.6% of variance was as follows: PCA model 1 = $(0.41 \times \text{maximum axial strain}) - (0.61 \times \text{percentage of low-intensity gray level}) - (0.68 \times \text{maximum axial shear strain magnitude})$, when each parameter was normalized to a mean value of 0 and an SD of 1. PCA model 1 had a mean value of 0.64 ± 1.35 for patients with symptomatic stenosis and -0.42 ± 0.74 for individuals with asymptomatic stenosis. Because the proportion of subjects with asymptomatic ICA stenosis who were treated for dyslipidemia was higher ($p = 0.008$) than that for subjects with

symptomatic stenosis (Table 1), the association of PCA model 1 with treatment for dyslipidemia was tested; no statistically significant difference was found ($p = 0.208$).

Discussion

New observations regarding elastography and confirmation of echogenicity results could be established in this pilot study, including the following observations. First, the maximum axial strain and axial shear of the ipsilateral carotids in patients with symptomatic ICA stenosis were lower than those for the index side of patients with asymptomatic stenosis. Second, the contralateral asymptomatic carotid sides of both patient groups for whom the degree of stenosis was approximately 25% provided elastography and echogenicity measures similar to those of the index side in patients with asymptomatic stenosis for whom

the mean degree of stenosis was greater than 70%. Third, echogenicity measures confirmed an association between the percentage of low-intensity gray levels of plaque and symptoms. Last, combining strain, shear, and echogenicity allowed optimization of classification accuracy with a sensitivity and specificity between 71% and 79%.

In the present study, we proposed a method to generate time-varying elastograms for carotid arteries stressed by the natural cardiac pulsation. The calculated elastography parameters can be seen in Figure S2 in an article by Roy Cardinal et al. [29]. Axial and lateral translations refer to displacements of the plaque within a cardiac cycle perpendicular to and along the carotid artery, respectively. Although reports have suggested that lateral (i.e., longitudinal) carotid wall motion could be related to cardiovascular risk [13, 14], we did not observe any association of ischemic symptoms with either of the plaque translation indexes.

The second parameter tested was axial strain, which corresponds to the orthogonal deformation for a long-axis vessel view. This parameter was previously correlated with MRI-based carotid plaque lipid content [15]. Axial strain rate (i.e., the time derivative of the axial strain) could also be related to MRI features of carotid plaque vulnerability [30]. To our knowledge, the association between reduced axial strain and symptoms was not established before the present study was conducted. Wang et al. [31] focused their analysis on subplaque regions with high axial strains. They determined correlations between deformation and a decline in cognitive performance in patients scheduled for endarter-

TABLE 4: Overview of Elastography Indexes Obtained for Plaques From the Ipsilateral or Index Side of Patients With Symptomatic or Asymptomatic Internal Carotid Artery Stenosis

Mechanical Parameter	Patients With Symptomatic Stenosis ($n = 26$)	Patients With Asymptomatic Stenosis ($n = 40$)	p^a
Cumulated axial translation (mm)	0.34 ± 0.24	0.34 ± 0.20	0.591
Cumulated lateral translation (mm)	0.96 ± 0.79	0.96 ± 0.57	0.609
Maximum axial strain (%)	1.88 ± 0.55	2.29 ± 0.50	0.003 ^b
Cumulated axial strain (%)	15.59 ± 6.76	15.35 ± 4.74	0.529
Maximum axial shear strain magnitude (%)	1.36 ± 0.29	1.53 ± 0.32	0.029 ^b
Cumulated axial shear strain magnitude (%)	12.74 ± 4.73	12.79 ± 3.77	0.618

Note—Except where otherwise indicated, data are mean (\pm SD) values. Elastography indexes were obtained from plaque regions containing 25% of highest pixel values.

^aComparison of index sides of patients with symptomatic stenosis versus those with asymptomatic stenosis, as assessed using t tests.

^bStatistically significant ($p < 0.05$).

ectomy. Although not significant, this latter study showed lower axial strains in patients with symptomatic stenosis versus asymptomatic stenosis when the whole plaque was analyzed, which is consistent with our results.

From a biomechanical point of view, elevated shear strain is considered important for initiating, stimulating, or spurring both aspects of development of the plaque into a rupture-prone plaque by means of fibrous cap weakening leading to ulceration [32, 33]. A shear pattern is obtained when deformation is neither parallel nor perpendicular to the long axis of the artery (i.e., angulated), because of tissue mechanical heterogeneity in advanced plaques. To our knowledge, an association between plaque axial shear and symptoms has also never been shown. In patients scheduled for endarterectomy for whom the degree of carotid stenosis is more than 60%, higher plaque axial shears were correlated with a decline in cognitive performance tests in both patients with symptomatic stenosis and patients with asymptomatic stenosis [34]. In the latter study, the possibility of using shear to distinguish symptoms was not reported.

Because vulnerable plaques are defined in histopathologic studies by the presence of soft lipid pools near the vessel lumen under a thin fibrous cap [3–5], one intuitively would predict that patients with symptomatic stenosis would have higher axial strains and shears. This prediction is the opposite of what we observed in the index side of patients with symptomatic stenosis, compared with patients with asymptomatic plaques with stenosis of low or high grades (Table 2). A few explanations may guide the interpretation of these results. First, a wide dispersion of lipid core areas has been associated with plaque rupture [35–37]. Our database could thus include small lipid pools and few subplaque areas with large deformation. This is indeed what was observed in a small subset of the current database in which MRI examinations were prescribed [15]. In that study, patients had fibrotic plaques with no prominent evidence of large lipid pools (mean lipid plaque volume was $9.6\% \pm 12.5\%$ for plaques considered to be vulnerable on the basis of MRI findings and $5.9\% \pm 10.8\%$ for nonvulnerable plaques).

A second explanation for the finding of lower strains and shears in patients with symptomatic stenosis may be that the lipid core embedded in a large plaque could behave as a damper reducing the deformation of the whole plaque. This explanation is supported by findings presented in Table S3 that show a negative correlation between the percentage of low-intensity gray level and the

cumulated axial strain ($p = 0.039$) or cumulated axial shear strain magnitude ($p = 0.011$). Finally, because the mean elapsed time between the first onset of symptoms and acquisition of an ultrasound scan was 22 ± 42 days, plaque healing and mechanical stress release after rupture may have occurred, thus reducing the whole plaque axial strain and shear. Plaque stabilization and remodeling represent a natural process after rupture [38], and our method could be sensitive to this phenomenon.

Any or a combination of the three aforementioned hypotheses may explain the lower deformations in the index plaque of patients with symptomatic stenosis. An additional analysis, which is reported in Table 4, was performed to keep only image pixels with large deformations attributed to the presence of soft lipid pools, as in previously published studies [16, 29]. Thresholds were applied on translation, strain, and shear strain elastograms to emphasize large mechanical movements. Pixel areas containing 25% of the highest values of each parameter were selected within the segmented areas of all image frames and were averaged over the whole sequence. As seen in Table 4, the index plaque of patients with symptomatic stenosis still showed smaller deformations, with the parameters maximum axial strain ($p = 0.003$) and maximum axial shear strain magnitude ($p = 0.029$) having a statistically significant difference between groups. This reprocessing of the data supports any of the three aforementioned hypotheses.

No clinical report based on ultrasound elastography has studied the natural evolution of carotid plaque biomechanics. Although intuitive and probable, an association between plaque biomechanics and rupture (stroke) remains to be proven. The whole question of the natural history of plaque progression and destabilization remains to be elucidated even if it is believed that atherosclerosis evolution is made of a succession of plaque stabilization and destabilization events [38]. To provide some insight regarding the role of plaque strain and shear on stroke events, a prospective longitudinal study design would be required. The same study design would be of interest to evaluate the stabilization of a rupture-prone plaque with the use of drug therapy.

Another limitation is the absence of histopathologic results to relate elastography and echogenicity biomarkers to the plaque content. This could have been feasible in patients with symptomatic stenosis treated by endarterectomy; however, our study design that included the untreated index sides of patients

with asymptomatic stenosis and the contralateral sides in both study populations precluded this possibility. Moreover, readers should be aware that pulse pressure, heart rate, and ultrasound frame rate are potential confounding variables for elastography that may contribute to the interpatient variability of those measurements. Indeed, the proposed method measures strain and shear produced by the natural pulsation of the artery between two consecutive image frames. However, as shown in Table 1, no differences between groups were present for systolic blood pressure, diastolic blood pressure, and heartbeat. The mean frame rate (expressed as images per second) was also similar between subjects with symptomatic stenosis (22.0 ± 4.0 images/s) and subjects with asymptomatic stenosis (21.9 ± 3.5 images/s) ($p = 0.736$). Although not a necessity for the present study, a practical way to eliminate these confounders would be to consider the pressure gradient between two consecutive images, with use of the following equation: pressure gradient = (systolic blood pressure – diastolic blood pressure) / [$60 \times (\text{frame rate} / \text{heartbeat})$]. In the current study, the mean pressure gradient (expressed as millimeters of mercury per image pair) was 3.73 ± 1.66 mm Hg for patients with symptomatic stenosis and 3.78 ± 1.47 mm Hg for patients with asymptomatic stenosis ($p = 0.807$). A linear interpolation of the pressure gradient to normalize elastography results could be applied to eliminate this confounder, if present.

As observed in Figures 1 and 2, intrapatient variability is observed on strain curves. Out-of-plane motion caused by the movement of the pulsating artery during the cardiac cycle may contribute to the noisy appearance of those strain curves. To reduce out-of-plane motion artifacts, compounding and time-ensemble approaches could be useful [39]. Higher temporal resolution is, however, necessary to apply these approaches. Finally, elastography computation could be problematic when ultrasound image quality is impaired by signal loss caused by severe calcification, attenuation resulting from the deep position of the carotid artery, or vessel tortuosity preventing the visualization of the plaque in a single imaging plane.

References

1. Virmani R, Kolodgie FD, Burke AP, Farb A, Schwartz SM. Lessons from sudden coronary death: a comprehensive morphological classification scheme for atherosclerotic lesions. *Arterioscler Thromb Vasc Biol* 2000; 20:1262–1275
2. Fleg JL, Stone GW, Fayad ZA, et al. Detection of high-risk atherosclerotic plaque: report of the NHLBI

- working group on current status and future directions. *JACC Cardiovasc Imaging* 2012; 5:941–955
3. Cheruvu PK, Finn AV, Gardner C, et al. Frequency and distribution of thin-cap fibroatheroma and ruptured plaques in human coronary arteries. *J Am Coll Cardiol* 2007; 50:940–949
 4. Naghavi M, Libby P, Falk E, et al. From vulnerable plaque to vulnerable patient, a call for new definitions and risk assessment strategies. Part I. *Circulation* 2003; 108:1664–1672
 5. Naghavi M, Libby P, Falk E, et al. From vulnerable plaque to vulnerable patient, a call for new definitions and risk assessment strategies. Part II. *Circulation* 2003; 108:1772–1778
 6. Lorenz MW, Polak JF, Kavousi M, et al. Carotid intima-media thickness progression to predict cardiovascular events in the general population (the PROG-IMT collaborative project): a meta-analysis of individual participant data. *Lancet* 2012; 379:2053–2062
 7. Den Ruijter HM, Peters SA, Anderson TJ, et al. Common carotid intima-media thickness measurements in cardiovascular risk prediction: a meta-analysis. *JAMA* 2012; 308:796–803
 8. Feinstein SB. Contrast ultrasound imaging of the carotid artery vasa vasorum and atherosclerotic plaque neovascularization. *J Am Coll Cardiol* 2006; 48:236–243
 9. Christodoulou CI, Pattichis CS, Pantziaris M, Nicolaides A. Texture-based classification of atherosclerotic carotid plaques. *IEEE Trans Med Imaging* 2003; 22:902–912
 10. Hashimoto H, Tagaya M, Niki H, Etani H. Computer-assisted analysis of heterogeneity on B-mode imaging predicts instability of asymptomatic carotid plaque. *Cerebrovasc Dis* 2009; 28:357–364
 11. Ainsworth CD, Blake CC, Tamayo A, Beletsky V, Fenster A, Spence JD. 3D ultrasound measurement of change in carotid plaque volume: a tool for rapid evaluation of new therapies. *Stroke* 2005; 36:1904–1909
 12. Wannarong T, Parraga G, Buchanan D, et al. Progression of carotid plaque volume predicts cardiovascular events. *Stroke* 2013; 44:1859–1865
 13. Svedlund S, Eklund C, Robertsson P, Lomsky M, Gan LM. Carotid artery longitudinal displacement predicts 1-year cardiovascular outcome in patients with suspected coronary artery disease. *Arterioscler Thromb Vasc Biol* 2011; 31:1668–1674
 14. Zahnd G, Vray D, Serusclat A, et al. Longitudinal displacement of the carotid wall and cardiovascular risk factors: associations with aging, adiposity, blood pressure and periodontal disease independent of cross-sectional distensibility and intima-media thickness. *Ultrasound Med Biol* 2012; 38:1705–1715
 15. Naim C, Cloutier G, Mercure E, et al. Characterization of carotid plaques with ultrasound elastography: feasibility and correlation with high-resolution magnetic resonance imaging. *Eur Radiol* 2013; 23:2030–2041
 16. Hansen HH, de Borst GJ, Bots ML, Moll FL, Pasterkamp G, de Korte CL. Validation of noninvasive in vivo compound ultrasound strain imaging using histologic plaque vulnerability features. *Stroke* 2016; 47:2770–2775
 17. Dempsey RJ, Vemuganti R, Varghese T, Hermann BP. A review of carotid atherosclerosis and vascular cognitive decline: a new understanding of the keys to symptomatology. *Neurosurgery* 2010; 67:484–493
 18. Grønholdt ML, Nordestgaard BG, Bentzon J, et al. Macrophages are associated with lipid-rich carotid artery plaques, echolucency on B-mode imaging, and elevated plasma lipid levels. *J Vasc Surg* 2002; 35:137–145
 19. Polak JF, Shemanski L, O'Leary DH, et al. Hypochoic plaque at US of the carotid artery: an independent risk factor for incident stroke in adults aged 65 years or older. Cardiovascular Health Study. *Radiology* 1998; 208:649–654
 20. Grønholdt ML, Nordestgaard BG, Schroeder TV, Vorstrup S, Sillesen H. Ultrasonic echolucent carotid plaques predict future strokes. *Circulation* 2001; 104:68–73
 21. Gupta A, Kesavabhotla K, Baradaran H, et al. Plaque echolucency and stroke risk in asymptomatic carotid stenosis: a systematic review and meta-analysis. *Stroke* 2015; 46:91–97
 22. Loizou CP, Pattichis CS, Pantziaris M, Kyriacou E, Nicolaides A. Texture feature variability in ultrasound video of the atherosclerotic carotid plaque. *IEEE J Transl Eng Health Med* 2017; 5:1800509
 23. Grant EG, Benson CB, Moneta GL, et al. Carotid artery stenosis: gray-scale and Doppler US diagnosis: Society of Radiologists in Ultrasound Consensus Conference. *Radiology* 2003; 229:340–346
 24. Destrempes F, Meunier J, Giroux MF, Soulez G, Cloutier G. Segmentation of plaques in sequences of ultrasonic B-mode images of carotid arteries based on motion estimation and a Bayesian model. *IEEE Trans Biomed Eng* 2011; 58:2202–2211
 25. Destrempes F, Meunier J, Giroux MF, Soulez G, Cloutier G. Segmentation in ultrasonic B-mode images of healthy carotid arteries using mixtures of Nakagami distributions and stochastic optimization. *IEEE Trans Med Imaging* 2009; 28:215–229
 26. Mercure E, Destrempes F, Roy Cardinal MH, et al. A local angle compensation method based on kinematics constraints for non-invasive vascular axial strain computations on human carotid arteries. *Comput Med Imaging Graph* 2014; 38:123–136
 27. Nicolaides AN, Kakkos SK, Kyriacou E, et al. Asymptomatic internal carotid artery stenosis and cerebrovascular risk stratification. *J Vasc Surg* 2010; 52:1486.e1–5–1496.e1–5
 28. Efron B, Tibshirani R. Improvements on cross-validation: the 0.632+ bootstrap method. *J Am Stat Assoc* 1997; 92:548–560
 29. Roy Cardinal MH, Heusinkveld MHG, Qin Z, et al. Carotid artery plaque vulnerability assessment using noninvasive ultrasound elastography: validation with MRI. *AJR* 2017; 209:142–151
 30. Huang C, Pan X, He Q, et al. Ultrasound-based carotid elastography for detection of vulnerable atherosclerotic plaques validated by magnetic resonance imaging. *Ultrasound Med Biol* 2016; 42:365–377
 31. Wang X, Jackson DC, Varghese T, et al. Correlation of cognitive function with ultrasound strain indices in carotid plaque. *Ultrasound Med Biol* 2014; 40:78–89
 32. Cinthio M, Ahlgren AR, Bergkvist J, Jansson T, Persson HW, Lindstrom K. Longitudinal movements and resulting shear strain of the arterial wall. *Am J Physiol Heart Circ Physiol* 2006; 291:H394–H402
 33. Idzenga T, Pasterkamp G, de Korte CL. Shear strain in the adventitial layer of the arterial wall facilitates development of vulnerable plaques. *Biosci Hypotheses* 2009; 2:339–342
 34. Wang X, Jackson DC, Mitchell CC, et al. Classification of symptomatic and asymptomatic patients with and without cognitive decline using non-invasive carotid plaque strain indices as biomarkers. *Ultrasound Med Biol* 2016; 42:909–918
 35. Rioufol G, Gilard M, Finet G, Ginon I, Boschat J, André-Fouet X. Evolution of spontaneous atherosclerotic plaque rupture with medical therapy: long-term follow-up with intravascular ultrasound. *Circulation* 2004; 110:2875–2880
 36. Kolodgie FD, Burke AP, Farb A, et al. The thin-cap fibroatheroma: a type of vulnerable plaque, the major precursor lesion to acute coronary syndromes. *Curr Opin Cardiol* 2001; 16:285–292
 37. Fujii K, Kobayashi Y, Mintz GS, et al. Intravascular ultrasound assessment of ulcerated ruptured plaques: a comparison of culprit and nonculprit lesions of patients with acute coronary syndromes and lesions in patients without acute coronary syndromes. *Circulation* 2003; 108:2473–2478
 38. Peeters W, Hellings WE, de Kleijn DPV, et al. Carotid atherosclerotic plaques stabilize after stroke: insights into the natural process of atherosclerotic plaque stabilization. *Arterioscler Thromb Vasc Biol* 2009; 29:128–133
 39. Porée J, Garcia D, Chayer B, Ohayon J, Cloutier G. Noninvasive vascular elastography with plane strain incompressibility assumption using ultrafast coherent compound plane wave imaging. *IEEE Trans Med Imaging* 2015; 34:2618–2631

FOR YOUR INFORMATION

A data supplement for this article can be viewed in the online version of the article at: www.ajronline.org.